Enhancing Motor Imagery EEG Classification Accuracy Using Weight Features Function

Abdel Fateh Doudou
Department of Electrotechnics, Setif 1 University-Ferhat Abbas, Algeria
abdelfateh.doudou@univ-setif.dz

Aicha Reffad
Department of Electrotechnics, Setif 1 University-Ferhat Abbas, Algeria
reffada@univ-setif.dz

Kamel Mebarkia
Department of Electronics, Setif 1 University-Ferhat Abbas, Algeria
kamel.mebarkia@rwth-aachen.de

Abstract: *Brain-Computer Interface (BCI) is a computerized system that gathers, analyzes, and translates neural signals into commands, which are then transmitted to an output device to perform certain tasks. One of the most difficult parts of the BCI Motor Imagery-Electroencephalogram (MI-EEG) based system is the Classification Accuracy (CA). In order to get accurate classification, efficient and rapid features extraction is required for developing a successful MI-EEG classification model. In this article, the Motor Imagery (MI) of Left-Hand (LH) and Right-Hand (RH) actions is recognized using the Weight Features Function (WFF) that transforms initial features into more discriminant features to feed a Support Vector Machine (SVM) classifier. Appropriate weights were chosen by the Genetic Algorithm (GA) optimization method. Applying optimized WFF to four different datasets (IIIb from BCI competition III, III from BCI competition II, 2b from BCI competition IV, and Open Brain-Machine Interface (OpenBMI) dataset) made significant improvements in the CA for all studied datasets. Before using the WFF technique, the initial CA for the four datasets was 90.1%, 95.71%, 86.73%, and 83.83%. After applying the WFF technique, the CA is improved and achieves 96.1%, 100%, 94.2%, and 88.70% respectively.*

Keywords: *brain-computer interface, features extraction, genetic algorithm, motor imagery, SVM classifier*.

Received January 1, 2025; accepted July 25, 2025
https://doi.org/10.34028/iajit/22/6/8

1. Introduction

Prospective Brain-computer interfaces (BCIs) are assistive technologies that enable users with disabilities to interact, communicate, and perform everyday tasks independently [3].

It is a computerized system that can be used to collect, analyze, and translate all aspects of mental activities and then convert them into commands that are sent to an output device to perform specific actions. Generally, we measure electrical activity using an Electroencephalogram (EEG), which uses electrodes placed on the scalp surface to collect the electrical activity resulting from activated neurons in the brain [39]. EEG is a non-invasive, portable, low-cost technique with high temporal resolution and easy-to-use [27]. Electrical current flows between neurons and generates wave patterns, commonly referred to as brain waves. Brain waves are classified into five distinct types: Delta [0.5-4 Hz], Theta [4-8 Hz], Alpha [8-12 Hz], Beta [12-30 Hz], and Gamma [>30 Hz]. Historically, these bands were classified through their unique characteristics such as morphology, topography, amplitude, frequency, reactivity, etc., [37].

Motor Imagery-Electroencephalography (MI-EEG) is one of the patterns used in BCI systems EEG based. MI-EEG involves imagining a movement, such as performing the action of waving a hand or stepping with a foot, without physically carrying out the movement and then measuring the brain activity associated with that movement [42]. This pattern of BCI can be used to control a computer or other electronic appliances, such as a robotic arm [28] or a wheelchair [34].

Interpreting brain activity from EEG signals is a major challenge for BCI systems because it requires sophisticated algorithms to accurately identify brain tasks from arrays of EEG signals. Furthermore, the identification of such tasks is often subjective, as different subjects might have different EEG signal representations for the same task, in addition to nonstationary, nonlinear, and noisy EEG signals with low spatial resolution. To overcome these challenges, researchers have devised numerous techniques to enhance the accuracy and reliability of the BCI system EEG-based. It involves extracting and selecting features that describe the relevant information from the EEG signals and then feeding these features to a pre-trained classifier that can identify the mental task class [7]. Thus, the accuracy of a BCI system relies largely on the extraction/selection of used features as well as the classifier.

Many techniques have been developed to extract features from MI-EEG signals. The most popular methods for extracting features from MI-EEG signals include Time-Frequency Representation (TFR), Fourier Transforms (FT) [12], Power Spectral Density (PSD) [9], Band-Power (BP) [2, 47], Wavelet Transform (WT) [18, 27] Common Spatial Patterns (CSP) [29, 40] and auto-regressive [32, 33]. Research has found that extracting the most relevant features for Motor Imagery (MI) tasks

from specific frequency bands is necessary to achieve better accuracy and efficiency [27, 32]. The rationale behind analyzing different frequency bands is that each band carries distinct types of information that can reveal specific patterns and aid in making predictions. For example, lower frequency bands such as Delta and Theta contain information related to sleep, memory consolidation, unconscious and meditative states [44]. In contrast, higher frequency bands such as Alpha and Beta are associated with wakefulness, attention, memory, and emotional states [8].

Extracting features from specific frequency bands allows more accurate and efficient identification of patterns and predictions relevant to MI tasks. Additionally, it can help for eliminating noise and irrelevant information that may be presented in the corresponding frequency band.

Many researchers have used the WT to perform MI-EEG classification [27, 36, 45]. The WT has been proven to be a powerful technique for the time-frequency analysis of non-stationary and quasi-stationary signals [36].

Most recent BCIs MI-EEG based are largely dependent on machine learning algorithms. A variety of classifiers are employed in this domain to recognize different MI tasks, such as Linear Discriminant Analysis (LDA), Support Vector Machine (SVM) with various kernel functions, decision tree (DT), and k-nearest neighbor (KNN), [3, 9, 12, 27, 30, 47].

You *et al*. [45] propose a novel method that combines Flexible Analytic Wavelet Transform (FAWT) and LDA to classify the MI-EEG signals as Left-Hand (LH) or Right-Hand (RH) movements on BCI competition III dataset IIIb and BCI competition II dataset III. Bashashati *et al*. [2] used a logistic regression algorithm as a classification method and employed wavelet features based on the mother wavelet morlet (BCI competition III dataset IIIb). Brodu *et al*. [7] used LDA to classify the MI-EEG signals and combined three kinds of features: BP, multifractal cumulants, and predictive complexity.

Deep learning models have become quite popular in BCI applications. They include Recurrent Neural Networks (RNNs) [11], Convolutional Neural Networks (CNNs) [23, 38], and Deep Belief Networks (DBNs) [35]. These models are known for their ability to extract intricate features from raw brain signals and their capacity to learn from vast amounts of data.

Salimpour *et al*. [38] propose a new approach to enhance the accuracy of classifying LH and RH in MI-EEG signals using Stockwell transform and CNN models on BCI competition II dataset III and BCI competition IV dataset 2b. Liu *et al*. [23] propose an end-to-end network called Compact Multi-Branch One-Dimensional Convolutional Neural Network (CMO-CNN) (BCI competition IV dataset 2b).

This work aims to improve the Classification Accuracy (CA) in BCI system MI-EEG signals. It uses a novel Weight Feature Function (WFF) to transform the proposed features into more discriminant features; so, the classifier identifies the MI of the LH and RH movements with higher accuracy. The WFF technique works by assigning a nonlinear function to polynomial weighted features extracted from the dataset. This double nonlinearity resulting from the WFF and the polynomial transformation is responsible for the discrimination of the resulting features. With the WFF, important features would be enhanced with higher weights contrary to less relevant features, which would be diminished by assigning lower weights. Overall, the WFF acts as pushing the classes to be more separable. The process of determining the suitable weights for each feature is performed by optimization using a Genetic Algorithm (GA). This study applies the WFF approach to four different datasets from the Open Brain-Machine Interface (OpenBMI) and BCI competition (dataset IIIb, dataset III, dataset 2b) and compares the results with the existing methods working for the same datasets to recognize hand movement either right or left.

2. Methodology

2.1. BCI System

The main purpose of the BCI technology is to accurately identify the subject's intended movements from their brain activity [1]. Figure 1 illustrates a block diagram of the BCI system. A subject imagines performing a motor action without carrying out any physical activity. The resulting EEG signals accompanying the action are firstly preprocessed and then reduced to features by extraction. Using a classifier, the MI action can be identified to control a variety of technological devices like computers, robotic arms, and wheelchairs via electronic interfaces.

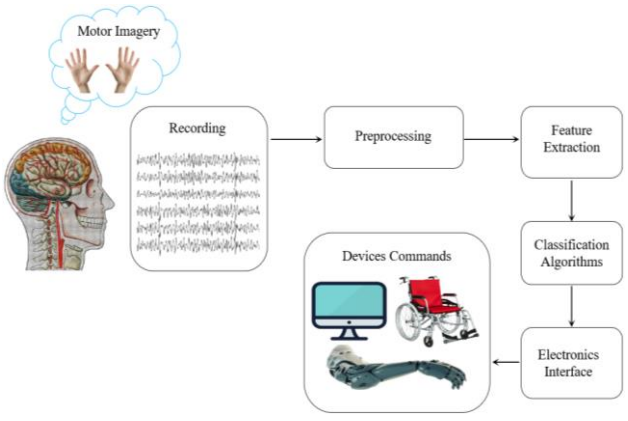

Figure 1. The general concept of a BCI system.

2.2. Dataset Description

Four publicly available datasets: the BCI competition III dataset IIIb (dataset 1) [5], the BCI competition II dataset III (dataset 2) [4], the BCI competition IV dataset 2b (dataset 3) [20], and the OpenBMI dataset (dataset 4) [19], were used in this study to evaluate the effectiveness

of the suggested approach. Table 1 contains details of the four datasets utilized in this work.

Table 1. A summary of the datasets utilized in this work.

Dataset	No. of subjects	No. of channels	No. of classes	No. of trials
Dataset 1	3	3	2	2480
Dataset 2	1	3	2	280
Dataset 3	9	3	2	6520
Dataset 4	54 (12)	62 (2)	2	10800

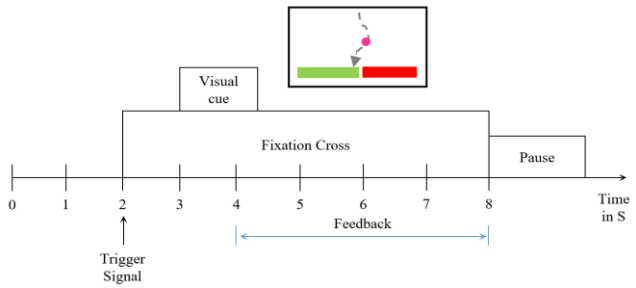

a) The timing scheme of dataset 1.

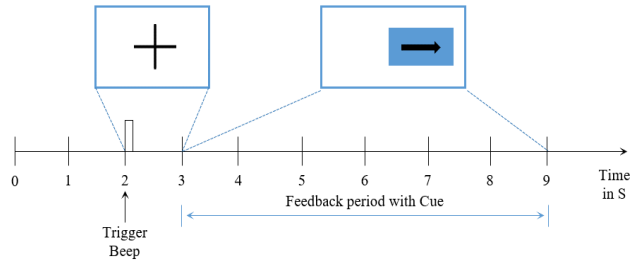

b) The timing scheme of dataset 2.

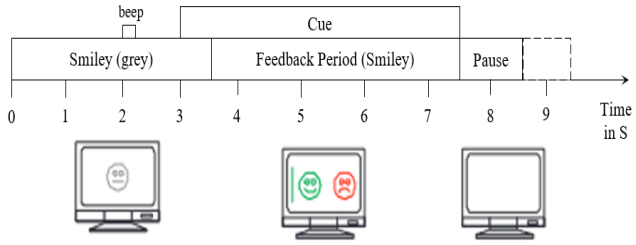

c) The timing scheme of dataset 3.

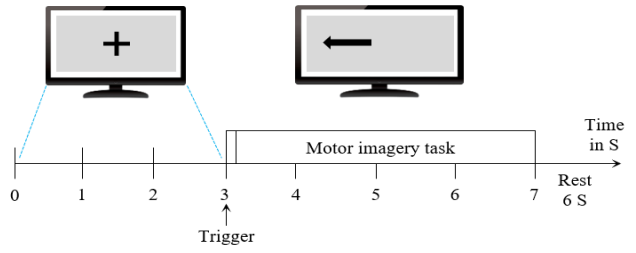

d) The timing scheme of dataset 4.

Figure 2. Timing scheme of the paradigm.

The details of these four datasets are described below.

- **Datasets 1**: this data set consists of two classes of MI-EEG data (LH and RH movements) from three subjects (O3, S4, X11). The experiment consists of three sessions for each participant and each session consists of four to nine runs. The number of trials is 320, 1080, and 1080 for participants O3, S4, and X11 respectively. The dataset was recorded over channels C3 and C4 using a bipolar EEG amplifier from G.tec. The EEG signals were sampled with 125 Hz, and filtered between 0.5 and 30Hz with a notch filter at 50 Hz. In this experiment, participants were instructed to imagine performing hand movements after hearing a beep sound. The instructions were to imagine moving either their LH or RH depending on randomly assigned cues. A graphical cue was displayed to the participant to provide feedback on his imagined action. The timing scheme for each trial is illustrated in Figure 2-a).
- **Datasets 2:** it contains two classes (LH/RH) of MI-EEG signals from a normal subject (25-year-old female referred to S1). During the recordings, the subject settled into a comfortable armchair and the cues for left and right were arranged randomly. In this experiment, there are a total of 7 runs, each comprising 40 trials (140 train trials and 140 test trials), lasting 9 seconds each. The timing scheme is shown in Figure 2-b). The recorded dataset was collected from three channels: C3, Cz, and C4 using a G.tec amplifier. The EEG signals were sampled with 128Hz, and filtered with a notch filter at 50 Hz, as well as a bandpass filter between 0.5 and 30 Hz. During the experiment, the subject was instructed to move a bar (on a screen) in the direction indicated by a given cue (left or right arrow) by feedback.
- **Dataset 3:** the dataset comprises information from a total of nine healthy subjects. EEG signals were recorded from three bipolar channels (C3, Cz, and C4) with a sampling frequency of 250 Hz. A bandpass filter ranging from 0.5 Hz to 100 Hz was applied to filter the signals, with an additional notch filter at 50 Hz. This dataset includes two types of MI paradigms, specifically focusing on the LH and RH movements. Each subject completed a total of five sessions, with the first two sessions consisting of training data obtained without feedback and including 120 trials per session. The remaining three sessions were recorded with feedback and included 160 trials per session. The experiment began with a gray smiley face appearing in the center of the screen at 0s. After 2s, a warning beep (1 kHz, 70 ms) was played, and between [3s, 7.5s] the subjects were instructed to imagine the movement of their LH or RH to move the smiley face to the left or to the right. The smiley face symbol on the screen would turn green if the subject imagined moving their LH or RH in the correct direction, but if they were incorrect, it would turn red. After 7.5s, the screen would turn blank, and a short break of 1s to 2s would be taken before continuing with the next trial. All trials followed the same pattern, as shown in Figure 2-c). In this study, the subjects of this dataset are referred to B01, B02… and B09.
- **Dataset 4:** the dataset consists of 54 subjects, recorded at a 1000 Hz sampling rate with 62 Ag/AgCl electrodes. It encompasses two MI classes, specifically LH and RH movements. The subjects were seated in a comfortable chair with armrests. Each subject underwent two sessions, each

comprising a training phase with 100 trials and testing phases with 100 trials, with balanced RH and LH imagery tasks. The timing scheme is depicted in Figure 2-d). in this study, we have selected only 12 subjects, specifically 'S04, S11, S20, S24, S25, S27, S34, S35, S40, S42, S46, S47,' based on their low accuracy in Lee *et al*. [19] to challenge our WFF method. To treat all datasets, the same way concerning features extraction, the channels C3 and C4 are also used for this dataset.

2.3. Pre-Processing

Pre-processing the dataset is an essential step in enhancing classification because it prepares the data for detailed analysis in the most effective and meaningful manner. First, because 'NaN' appears in the subjects O3, S4, X11, and B06, we deleted all trials that have missing data represented by 'NaN'. After this process, the size of the datasets became 160 examples for O3, 536 for S4, 539 for X11, and 318 examples for subject B06. By doing so, all datasets used in the analysis were valid without missing data that could influence the results. Furthermore, two second-order Butterworth band pass filters were used to enhance the chances of discovering distinctive features in signals SC3 and SC4 which are from the channels C3 and C4 respectively. The frequency bands selected for this analysis are B1 ([7-24] Hz), and B2 ([25-29] Hz). Thereby, four distinct signals are obtained for each trial. These signals are named SC_{31}, SC_{32}, SC_{41}, and SC_{42} (see Figure 4).

2.4. Features Extraction

The process of extracting information from a given set of data is known as feature extraction. It is a critical step in making the data more understandable for the machine learning algorithm. In fact, features extraction can be accomplished in three ways: frequency domain, time domain, and frequency-time domain. The features used in this work are very diversified. In fact, features from the frequency domain, time domain, and time-frequency domain (Continuous Wavelet Transform (CWT) and Discrete Wavelet Transform (DWT)) for MI-EEG signals are extracted in order to identify the RH/LH movement that will be used in the BCI system.

2.4.1. Wavelet Transform

Due to the non-stationary nature of the EEG signals [27], the WT approach is a good option, for the reason that it handles the time-frequency domain aspect. WT is very important in signal processing and is often used in two ways:

a) CWT: it measures the similarity between a signal and an analytical function called a mother wavelet using inner products. The CWT formula for a signal *x(t)* is given by:

$$C_x(a,b) = \frac{1}{a}\int_{-\infty}^{\infty} x(t)\Psi\left(\frac{t-b}{a}\right)dt \quad (1)$$

Where a is a scale parameter and b is a parameter for the position of the mother wavelet Ψ in time.

b) DWT: the DWT requires two filters to split the signal into different levels: a low-pass filter and a high-pass filter. The low-pass filter returns the Approximation coefficient (A1), while the high-pass filter returns the Detailed coefficient (D1). The approximation signal is divided again into several levels of lower-resolution components. Figure 3 illustrates the DWT decomposition of the digital signal $x[n]$ till the third level.

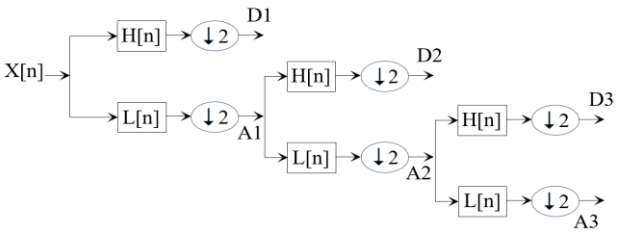

Figure 3. Wavelet decomposition of DWT till the third level.

The first level is expressed mathematically as:

$$A[k] = \sum_n x[n].L[2k-n] \quad (2)$$

$$D[k] = \sum_n x[n].H[2k-n] \quad (3)$$

Where $x[n]$ is the signal, $A[k]$ and $D[k]$ are the approximation and the detailed coefficients respectively. The functions $L[n]$ and $H[n]$ represent the filter coefficients, and n represents the sampling point of the signal. In this work, EEG signals were decomposed to the third level using biorthogonal 3.3 filters.

2.4.2. Other Diversified Features

The distribution of a signal's power content over frequencies is called the PSD. The following formula is used to calculate the PSD of a signal $x(t)$:

$$P_x(f) = |fft(x^2)| \quad (4)$$

Where f is the frequency, while Fast Fourier Transform (FFT) stands for the fast TF algorithm.

The variance of EEG signal (var) is useful for determining signal power and can be stated as:

$$var = \frac{1}{N-1}\sum_{i=1}^{N}(x_i)^2 \quad (5)$$

Where x is the signal and N is the length of the signal.

Skewness measures the asymmetrical distribution of a signal around its mean or median value. Kurtosis is defined as the average fourth power of a signal's deviation from its mean value divided by the standard deviation's fourth power. The skewness and Kurtosis are given by Equations (6) and (7).

$$skew = \frac{1}{N\sigma^3}\sum_{n=1}^{N}(x_n - \mu)^3 \quad (6)$$

$$kurt = \frac{1}{N\sigma^2}\sum_{n=1}^{N}(x_n - \mu)^4 \quad (7)$$

Where σ is the standard derivation of the random variable x and μ represents its mean.

Root Mean Square (RMS) is calculated by the following equation:

$$RMS = \sqrt{\frac{1}{N}\sum_{i=1}^{N}(x_i)^2} \quad (8)$$

Enhanced Wave-Length (EWL) and Enhanced Mean Absolute Value (EMAV) are calculated by Equations (9) and (10).

$$EWL = \sum_{i=2}^{N}|(x_i - x_{i-1})^P| \quad (9)$$

$$EMAV = \frac{1}{N}\sum_{i=1}^{N}|(x_i)^P| \quad (10)$$

$$P = \begin{cases} 0.80, & if \ \ 0.3N \ \ \leq i \leq 0.7N \\ 0.50, & otherwise \end{cases} \quad (11)$$

The parameter *P* in Equation (11) is utilized to determine the effect of the sample within the signal, as shown in Equations (9) and (10). A higher number of *P* is used in 30% to 70% of areas in EMAV and EWL [43].

Mean Curve Length (*MCL*) measures signal complexity and irregularity and is given by Equation (12).

$$MCL = \frac{1}{N}\sum_{i=2}^{N}|x_i - x_{i-1}| \quad (12)$$

Mean Energy (*ME*) is useful for determining signal power and is given by Equation (13)

$$ME = mean(x^2) \quad (13)$$

First Difference (*FD*) helps in the analysis of signal patterns and trends and is given by Equation (14).

$$FD = \frac{1}{N-1}\sum_{i}^{N-1}|x_{i+1} - x_i| \quad (14)$$

In the present study, we extract relevant features from specific frequency bands. Once the features have been extracted, they are combined to form a single features vector. This vector contains information from time and frequency and conjoint time-frequency domains. This diversity from different domains aims to improve the CA of the MI brain tasks.

A flowchart of the signal processing steps and the corresponding extracted features is shown in Figure 4. Using two pass-band filters, with the indicated pass bands, the two EEG signals of the two channels C3 and C4 generate four signals (SC_{31}, SC_{32}, SC_{41}, SC_{42}). To take the spatial information into account, all proposed features were a ratio between features of signals obtained from channel C3 (SC_{3i}; i=1, 2) and features of signals obtained from channel C4 (SC_{4i}; i=1, 2). In fact, 84 features were proposed. The first 42 features are indicated and defined in Table 2. The remaining 42 features are exactly the reverse of the first 42 features. For example, f_{43} is f_1^{-1} and f_{44} is $f_2^{-1}$and so on.

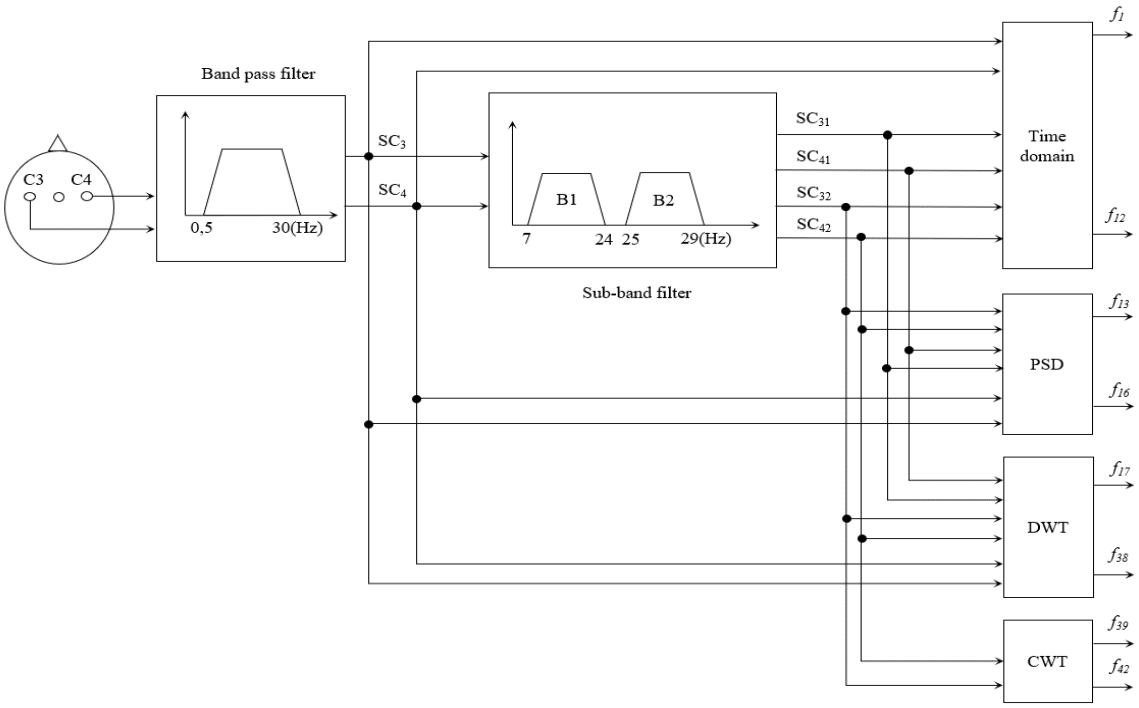

Figure 4. Flowchart of the signal processing with features extraction.

The reverse approach, as a nonlinear transformation, permits more diversity in features so the MI-EEG brain tasks can be represented differently; consequently, their identification could be more accurate.

Table 2. Proposed features and their expressions.

Features	Expressions
$\mathbf{f_1}$	$MCL(SC_{31})/MCL(SC_{41})$
$\mathbf{f_2}$	$sum(SC_3)/sum(SC_4)$
$\mathbf{f_3}$	$mad(SC_{31})/mad(SC_{41})$
$\mathbf{f_4}$	$ME(SC_{31})/ME(SC_{41})$
$\mathbf{f_5}$	$FD(SC_{32})/FD(SC_{42})$
$\mathbf{f_6}$	$kurt(SC_3)/kurt(SC_4)$
$\mathbf{f_7}$	$\left(\frac{sum(SC_3^{\,2})}{length(SC_3)}\right)/\left(\frac{sum(SC_4^{\,2})}{length(SC_4)}\right)$
$\mathbf{f_8}$	$\left(\frac{mean(SC_3^{\,2})}{length(SC_3)}\right)/\left(\frac{mean(SC_4^{\,2})}{length(SC_4)}\right)$
$\mathbf{f_{j+8}}$	$\left(\frac{mean(SC_{3j}^{\,2})}{length(SC_{3j})}\right)/\left(\frac{mean(SC_{4j}^{\,2})}{length(SC_{4j})}\right)\ j=1\ldots2$
$\mathbf{f_{j+10}}$	$\left(\frac{rms(SC_{3j}^{\,2})}{length(SC_{3j})}\right)/\left(\frac{rms(SC_{4j}^{\,2})}{length(SC_{4j})}\right) j=1\ldots2$
$\mathbf{f_{13}}$	$var(P_3)/var(P_3+P_4)$
$\mathbf{f_{14}}$	$max(P_3)/max(P_4)$
$\mathbf{f_{15}}$	$kurt(P_{31})/var(P_{41})$
$\mathbf{f_{16}}$	$kurt(P_{31})/median(P_{41})$
$\mathbf{f_{17}}$	$STD(D3_{32})/STD(D3_{42})$
$\mathbf{f_{18}}$	$skew(D1_{32})/skew(D1_{42})$
$\mathbf{f_{j+17}}$	$kurt(Dj_{32})/kurt(Dj_{42})$ j=2,3
$\mathbf{f_{21}}$	$sum(D3_{32}^2)/sum(D3_{42}^2)$
$\mathbf{f_{j+20}}$	$MCL(Dj_{32})/MCL(Dj_{42})$ j=2,3
$\mathbf{f_{24}}$	$mad(D3_{32})/mad(D3_{42})$
$\mathbf{f_{j+24}}$	$EWL(Dj_{32})/EWL(Dj_{42})$ j=1…3
$\mathbf{f_{28}}$	$EMAV(D2_{32})/EMAV(D2_{42})$
$\mathbf{f_{29}}$	$sum(A1_3^2)/sum(A1_4^2)$
$\mathbf{f_{30}}$	$mean(\lvert A1_{32}\rvert)/mean(\lvert A1_{42}\rvert)$
$\mathbf{f_{31}}$	$rms(\lvert A1_{31}\rvert)/rms(\lvert A1_{41}\rvert)$
$\mathbf{f_{32}}$	$median(\lvert A1_{32}\rvert)/MCL(\lvert A1_{42}\rvert)$
$\mathbf{f_{33}}$	$EWL(A1_3)/EWL(A1_4)$
$\mathbf{f_{j+33}}$	$EWL(A1_{3j})/EWL(A1_{4j})$ j=1,2
$\mathbf{f_{36}}$	$EMAV(A1_3)/EMAV(A1_4)$
$\mathbf{f_{37}}$	$EMAV(A1_{32})/EMAV(A1_{42})$
$\mathbf{f_{38}}$	$max(A1_3)/max(A1_4)$
$\mathbf{f_{i+37}}$	$\frac{sum(C_{SC32}(i,:)^2)}{sum(C_{SC42}(i,:)^2)}\ i=2\ldots5$

The diversification of features depends on the frequency content of the signals from which they are extracted, with distinct allocations for different frequency ranges: 20 features are designated for frequencies spanning from 0.5 to 30 Hz, 18 features are specified for frequencies ranging between 7 and 24 Hz, and a larger set of 46 features is designated for frequencies between 25 and 29 Hz.

2.5. Features Selection

Due to the diversity of the proposed features, the carried information about the brain tasks can be redundant or shared between a group of features. Efficient BCI system needs relevant features with fewer numbers to speed up the identification phase. To this end, the feature selection is performed by optimization using GA [31].

2.6. Weight Features Function (WFF)

The problem of the brain tasks identification is very difficult due to the complicated nature of the EEG signals carrying the task information. In fact, they are nonlinear, non-stationary, and undergo variations not just for extra-subjects but also for intra-subjects. To get better classification, classes should be distinguishable by features.

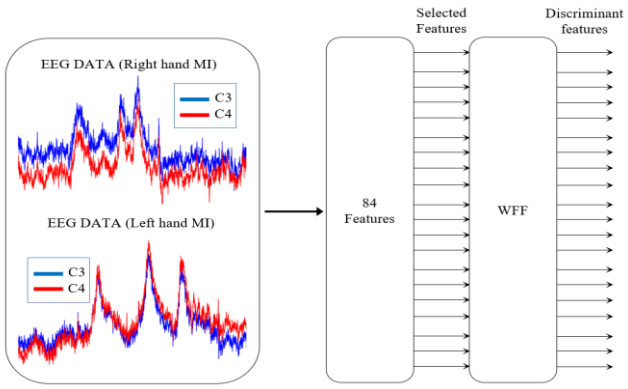

Figure 5. EEG signals illustration for LH/RH actions with discriminant features extracted by WFF.

For this purpose, Selected Features (SF), in the first phase, need further processing to be more discriminant. In this work, SF were transformed by a double nonlinearity performed by the following WFF:

$$X_i' = WFF(X_i) = tan\left(w_{1i} + w_{2i}X_i + w_{3i}X_i^2\right) \quad (15)$$

Where i=1…SF. For each feature *Xi* among the SF, three weights (w_{1i}, w_{2i}, w_{3i}) should be tuned in a way the resulting feature *Xi'* by the tangent function 'tan' would be discriminant. The weights tuning is performed by GA optimization subject to minimization of the misclassification rate. The periodicity of the 'tan' function permits to transform non-linearly sub-regions of the learning examples not necessarily equilateral due to the polynomial nonlinearity. This WFF acts as the kernel function of the SVM classifier, but it keeps the same dimension. So, this WFF tries to make classes more separable, making the SVM classifier function easier afterward. Figure 5 illustrates the EEG signal for LH/RH movements highlighting discriminant features extracted through WFF.

2.7. SVM Classifier

Due to its high accuracy in predicting the class of a given dataset, SVM has become one of the most popular discriminative classification models for nonlinear and linear classifications. It's a supervised learning algorithm that helps classify data points by finding a hyperplane in a high-dimensional space that best separates different classes in a dataset [43, 46, 47]. The hyperplane is chosen to maximize the margin between the two closest data points of different classes, which leads to a highly accurate classification of new data points. The data points nearest to the hyperplane are known as support vectors, and they play an important role in the determination of the decision boundary. The SVM classifier is a powerful tool for classification and regression tasks and is being employed to identify various MI-EEG signals [27, 47].

3. Results

In this study, four different datasets were used to perform

LH/RH movement recognition. The dataset 1 (Dataset IIIb) has three subjects. The dataset 4 has 12 subjects. The CA for these two datasets is performed by a 10-fold cross-validation technique to avoid biased evaluation. The CA for the dataset 2 (dataset III) that has one subjects and the dataset 3 (dataset 2b) that has 9 subjects is performed by the holdout evaluation technique that is imposed by the datasets i.e., datasets are already divided into two parts: train part and test part. The results for all datasets are presented in many stages as follows:

1. The classification is performed with all 84 features using three kinds of classifiers (SVM, KNN, LDA).
2. Using the best classifier from the last results Linear SVM (LSVM), firefly optimization is performed to find the best processing duration for each subject.
3. The classification is performed by suitable features selected by GA for each subject.
4. The SF are subject to weighting using the proposed WFF technique to improve the CA. The best weights for SF are optimized also by GA. At the end, we evaluate our approach by comparing them to existing methods that have used the same databases 'dataset 1, dataset 2, dataset 3, and dataset 4.'

3.1. CA with All Features

Table 3 represents the CA of the four datasets and the corresponding mean with respect to different classifiers (SVM, KNN, and LDA). By trial and error, the beginning time is set to 3.85s and the processing duration is set to 1 s.

Table 3. CA using indicated classifiers for all datasets.

Datasets	Subjects	Classifiers		
		LSVM	KNN	LDA
Datasets 1	O3	75.8	74.4	71.9
	S4	76.7	74.1	73.7
	X11	76.9	74.2	73.8
Mean (%)		76.47	74.2	73.1
Datasets 2	S1	82.1	80.7	82.1
Datasets 3	B01	68.1	65.6	65
	B02	52.2	51.8	52
	B03	59.4	55	52
	B04	91.4	90.5	91
	B05	81.4	81.6	80
	B06	71.3	66.3	68.8
	B07	66.3	61.9	64.1
	B08	77.4	73.2	75.3
	B09	72.8	74.2	75.3
Mean (%)		71.14	68.9	69.49
Datasets 4	S04	75	73	75
	S11	75	74.3	74.5
	S20	75	71.3	74.8
	S24	75.8	74	75
	S25	76	75	75
	S27	77.3	77.8	76.3
	S34	76.5	74.3	75
	S35	85	78	79.5
	S40	79.5	75	79.3
	S42	79.8	77.8	78
	S46	75	74.3	75
	S47	75	76.8	75.3
Mean (%)		77.07	75.13	76.05

From Table 3, the LSVM classifier is the best one for all datasets with a CA mean of 76.5%, 82.1%, 71.14%, and 77.07% for dataset 1, dataset 2, dataset 3, and dataset 4 respectively. Consequently, the remaining classification results are performed by the LSVM classifier.

3.2. CA with Tuned Processing Durations

Due to the non-stationary nature of the EEG signals, features that carried the LH/RH movement information are very sensitive to the processing duration i.e., the duration of the segment by which the features are calculated. For this reason, processing durations for each subject are tuned by the firefly optimization technique [21]. Using the best classifier found previously LSVM while maintaining the start time position unchanged (3.85s). Table 4, lists the CA for all subjects with respect to the best processing duration found by the firefly algorithm.

As we can see, from Table 4, most processing durations are longer than 1.5s. These processing durations will be used for the coming results.

Table 4. CA (%) for all subjects with respect to the best processing duration found by the firefly optimization algorithm.

Datasets	Subjects	Processing duration (s)	CA (%)
Datasets 1	O3	1.8720	76.13
	S4	3.5047	84.29
	X11	3.4420	80.43
Datasets 2	S1	3.6056	90
Datasets 3	B01	0.5981	68.43
	B02	2.8743	60.71
	B03	0.8054	64.68
	B04	1.8122	95
	B05	2.2322	90.29
	B06	3.4624	84.27
	B07	0.7429	72.18
	B08	2.2914	91.87
	B09	3.2189	90.93
Datasets 4	S04	0.4187	79.25
	S11	0.7440	78.5
	S20	1.5449	80.5
	S24	0.6414	79.5
	S25	0.8355	78.75
	S27	3.7015	80
	S34	1.7820	79.75
	S35	0.5322	88.75
	S40	2.1925	79.5
	S42	2.0043	79.75
	S46	0.3359	79.25
	S47	0.8034	79.5

3.3. CA with Selected Features

Arriving now, at the selection of features to choose the most relevant ones. To do so, GA optimization is used to minimize the misclassification rate (classification error). The GA should select a suitable group of features among 2^{84} possible groups. Table 5, represents the CA of the four datasets before and after the features selection with their number (SF). Overall, the number of the SF is reduced by about 60%. The average CA is improved by about 10% for dataset 1 and about 5% for the remaining datasets. Features selection discards redundant features and non-discriminant ones.

Figure 6 demonstrates the GA optimization for choosing suitable features for some subjects (one subject from each dataset). A CA of 92.53% (100-7.46), 95.71 %, 98.23 %, and 92 % is reached using 35, 42, 35, and 21 features for the indicated subjects respectively.

Table 5. CA (%) for the four datasets before and after features selection with indicated SF number.

Datasets	Subjects	All features (84)	Mean (%)	SF	Mean (%)
Datasets 1	O3	76.13	**80.29**	92.53 (35)	**90.1**
	S4	84.30		90.32 (37)	
	X11	80.44		87.45 (35)	
Datasets 2	S1	90	**90**	95.71 (42)	**95.71**
Datasets 3	B01	68.43	**79.82**	75.5 (30)	**86.73**
	B02	60.71		71.78 (30)	
	B03	64.68		75 (44)	
	B04	95		98.23 (35)	
	B05	90.29		94.41 (39)	
	B06	84.27		89.3 (34)	
	B07	72.18		82.5 (31)	
	B08	91.87		96.25 (21)	
	B09	90.93		95.62 (21)	
Datasets 4	S04	79.25	**80.25**	82 (29)	**83.83**
	S11	78.5		81.5 (31)	
	S20	80.5		84.5 (38)	
	S24	79.5		85.75 (27)	
	S25	78.75		84.25 (22)	
	S27	80		82.5 (38)	
	S34	79.75		83.5 (21)	
	S35	88.75		92 (21)	
	S40	79.5		83.5 (32)	
	S42	79.75		83 (36)	
	S46	79.25		82.25 (21)	
	S47	79.5		81.25 (36)	

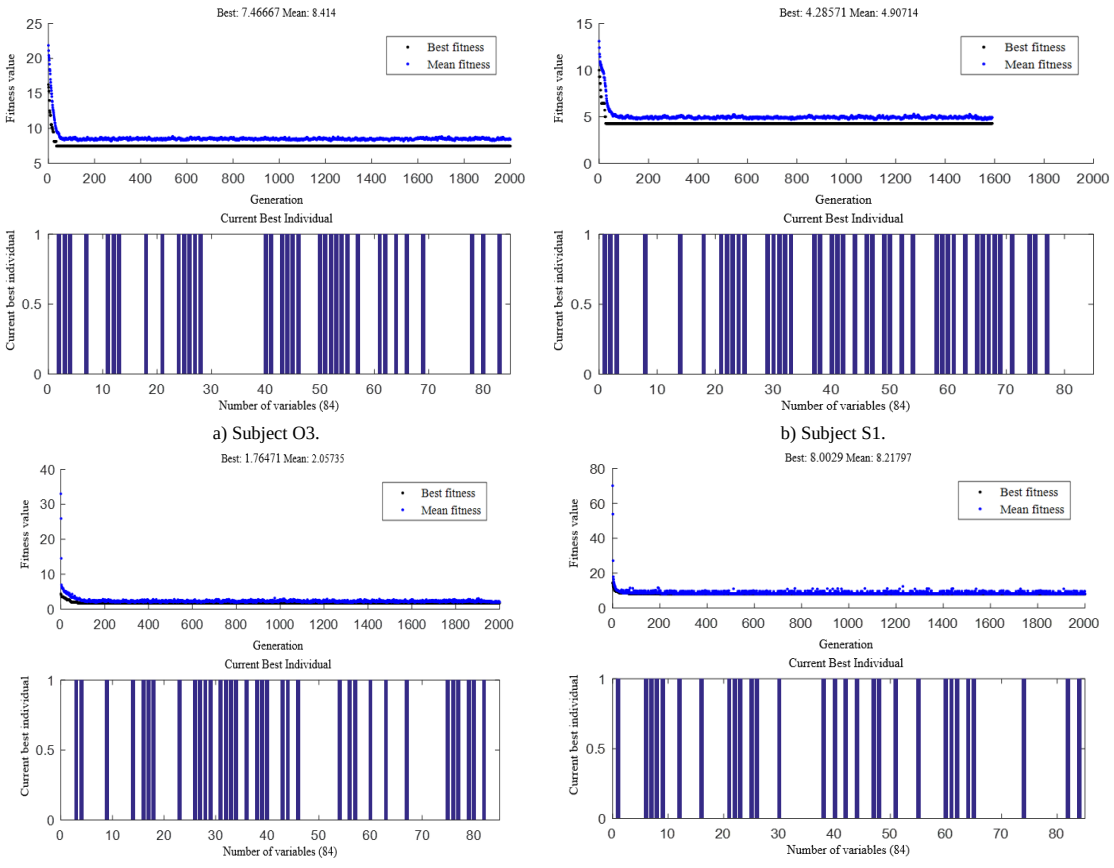

a) Subject O3.

b) Subject S1.

c) Subject B04.

d) Subject S35.

Figure 6. Features selection using GA optimization for the indicated subjects.

3.4. CA Using the WFF Technique

To enhance further the CA of LH movement, the last SF will undergo a weighting operation using the WFF technique. The GA is used to find suitable weights for each feature. According to the WFF expression 'Equation (15)', the GA should find three weights for each feature i.e., the number of weights to be found is three times the number of features.

Table 6. CA (%) and their mean over the dataset after weighting by the WFF techniques.

Datasets	Subjects	Using WFF	Mean (%)
Datasets 1	O3	100	96.1
	S4	95.48	
	X11	92.81	
Datasets 2	S1	100	100
Datasets 3	B01	84.68	94.2
	B02	85	
	B03	87.81	
	B04	100	
	B05	100	
	B06	99.05	
	B07	92.18	
	B08	100	
	B09	99.06	
Datasets 4	S04	86.25	88.70
	S11	86.75	
	S20	88	
	S24	88.75	
	S25	88.5	
	S27	87.75	
	S34	87.75	
	S35	97	
	S40	88.25	
	S42	90	
	S46	88.25	
	S47	87.25	

The CA of LH/RH movements for all subjects using optimized weights in the WFF technique are presented in Table 6. It is clear that the use of the WFF technique has improved the CA accuracy in all subjects. To get a clear idea about the contribution of WFF techniques, the average of CA for each dataset before and after using the WFF technique is presented as a 'bar' plot in Figure 7.

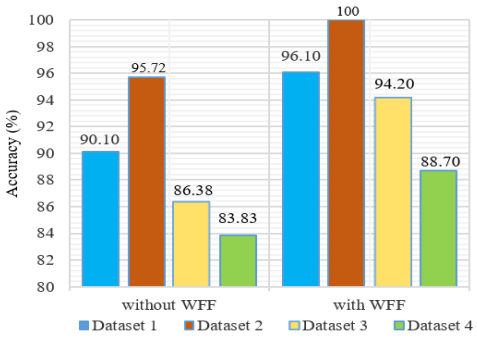

Figure 7. CA for the four datasets before and after applying the WFF weighting.

It is clear from Figure 7 that the CA has been significantly improved. In fact, the mean CA increases from 90.10% to 96.10%, from 95.72 % to 100%, from 86.38% to 94.2%, and from 83.83% to 88.70% with and without WFF technique for the four datasets respectively. These results indicate an improvement of about 5% in all datasets. Without a doubt, the WFF weighting is an efficient technique to make features more discriminant leading to a significant improvement in the LH/RH movement identification.

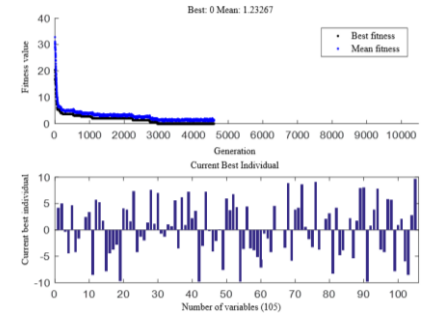

a) Subject O3.

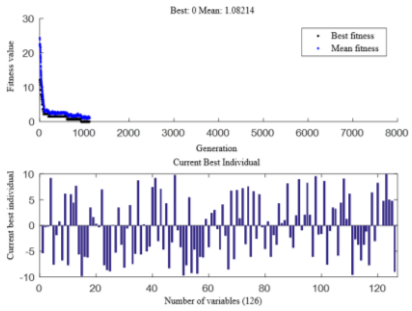

b) Subject S1.

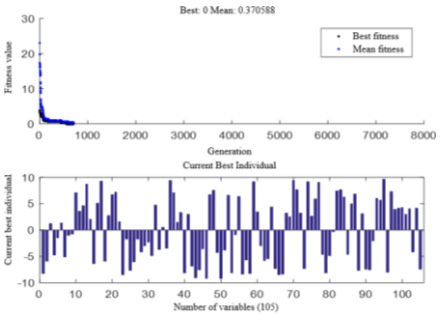

c) Subject B04.

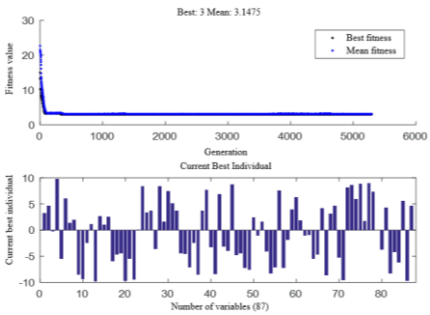

d) Subject S35.

Figure 8. GA optimization of weights in WFF technique for the indicated subjects.

Figure 8 represents the GA optimization process for some results of Table 6. It represents the GA optimization of the weights in the WFF technique for four subjects, one subject from each dataset.

We have to mention that other non-linear functions were used in the WFF expression like 'asin', 'sinc', 'cos', 'acos', and 'atan' functions trying to find a better CA, but we could not find a CA better than the CA given by the 'tan' function which gives a mean CA of 96.1%, 100%, 94.2% and 88.70% for the four datasets respectively.

To get a clear idea about the left/right classification using the LSVM classifier, the confusion matrices of the classification in four datasets are represented as mean in Figure 9. As the datasets are not imbalanced data, the confusion matrices indicate that there is no confusion in

the recognition of the LH and the RH movement i.e., there is no difference in the LH and the RH movement recognition. That means, the proposed technique WFF produces more sensitive and discriminant unconfused features.

The GA parameters used in the optimization process are indicated in the Table 7.

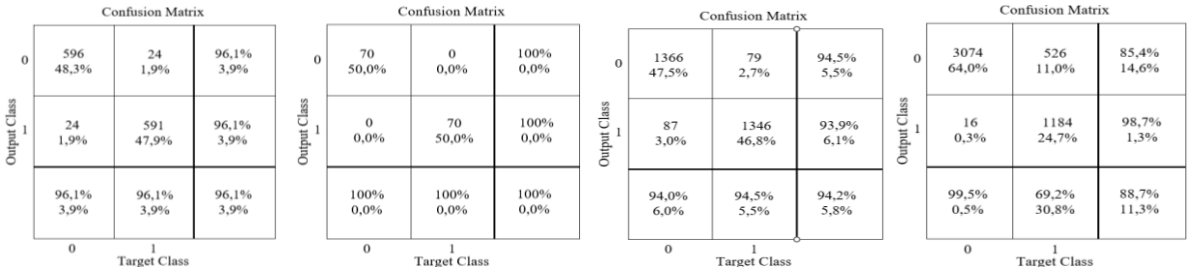

a) Dataset 1. b) Dataset 2. c) Dataset 3. d) Dataset 4.

Figure 9. Confusion matrices for the four datasets.

Table 7. GA characteristics used in the optimization.

Parameters	Definition or value
Population type	Bit string / double victor
Population size	200
Scaling function	Shift linear
Selection function	Remainder
Mutation function	Constraint dependent
Generations	2000/10000
Elite count	0.05*Population size
Crossover fraction	0.8
Crossover function	Constraint dependent
Migration direction	Forward
Migration fraction/interval	0.2/20
Termination criteria	Stall generations=5000

3.5. CA Comparison with Existing Methods

Due to the importance of the BCI technology, several researches have been developed new techniques in order to identify accurately brain tasks using MI-EEG signals. To see how our method performs in LH/RH movement classification with respect to the existing works while using the same datasets (dataset 1, dataset 2, dataset 3, and dataset 4), Table 8 summarizes the CA of the existing works with their methods and their features with respect to our work. As we can see, our method outperforms all existing methods in all datasets. The best CA for dataset 1 was 94.11% using multi-classification of three optimized SVM classifiers [27]. Although multi-classification boosts the CA, our method outperforms this multi-classification using just one LSVM classifier with a CA of 96.1%. Using the CNN classifier (deep learning), the CA for the dataset 2 was 99.29% [38]. In our work, the CA achieves 100%. Concerning the dataset 3, our method is more accurate than the one performed by the CNN classifier (deep learning-based transfer learning) which was 89.02% [38], with an improvement of about 5% (94.2%). Although in the dataset 4 our method achieves a CA of 88.70% which is more than the one found by Lee *et al*. [19] with 51.98% CA; in the later method, they utilized CSSP features with 20 channels and an LDA classifier. Using just two electrodes to find such performance (36% more) is really a noteworthy result.

Table 8. Summary of the CA (%) with indicated features and classifiers for works that used dataset 1, dataset 2, dataset 3, and dataset 4.

Datasets	Works	Features	Classifiers	Mean (%)
Dataset 1	Lotte *et al*. [24]	Band power	SVM	79.36
	Zhong *et al*. [47]	Band power	VB	78.96
	Brodu *et al*. [6]	Wavelet features (Morlet)	LDA	80.95
	Brodu *et al*. [7]	BP, Multifractal, Complexity	LDA	81.30
	Bashashati *et al*. [2]	Wavelet features (Morlet)	LR	81.47
	Chen *et al*. [10]	TQWT	LDA	81.75
	You *et al*. [45]	FAWT	LDA	86.66
	Mebarkia and Reffad [27]	16 Diversified features	Three optimized SVMs	94.11
	This work	**84 Diversified features with optimized WFF**	**SVM**	**96.1**
Dataset 2	Liu *et al*. [22] SVM	Common spatial pattern (CSP)	SVM	82.86
	Jang *et al*. [15]	STFT	KNN	83.57
	Khasnobish and Bhattacharyya [17]	Average band power of alpha and beta	KNN	84.29
	Chen *et al*. [10]	TQWT	LDA	88.11
	Tabar and Halici [41]	STFT	Deep learning	90
	You *et al*. [45]	FAWT	LDA	94.29
	Kant *et al*. [16]	CWT Filter-bank	Deep Transfer-learning	95.71
	Salimpour *et al*. [38]	CNN-based features from Stockwell TFM	SVM	99.29
	This work	**84 Diversified features with optimized WFF**	**SVM**	**100**
Dataset 3	Degdevir *et al*. [13]	Hjorth algorithm	SVM	82.58
	Han *et al*. [14]	STFT	PCNN	83
	Malan *et al*. [26]	Dual-tree complex wavelet, NCA	SVM	84.02
	Lu *et al*. [25]		Deep learning based on restricted Boltzmann machines	84.2
	Liu *et al*. [23]		CMO-CNN	87.19
	Salimpour *et al*. [38]	CNN-based features from Stockwell TFM	SVM	89.02
	This work	**84 Diversified features with optimized WFF**	**SVM**	**94.2**
Dataset 4	Lee *et al*. [19]	CSSP	LDA	51.98
	This work	**84 Diversified features with optimized WFF**	**SVM**	**88.70**

Our method dominates all existing methods for all datasets. That means the WFF technique using 'tan' function is a good alternative to transfer the classification problem to be more linearly separable with the new transferred features.

4. Conclusions

The complex nature of the EEG signal, its variability intra-subject and extra-subjects, and the synchronization problem all make brain tasks identification hard for the BCI system. In this paper, we have proposed 84 diversified novel features to identify the LH/RH movement using a LSVM classifier from MI-EEG signals. To enhance the CA, we selected relevant features and weighted them using the GA optimization algorithm. Using the WFF technique approach, which transforms the SF into more discriminant ones, the CA was improved significantly. After evaluating our approach on public BCI competition databases and OpenBMI, the best accuracy of 96.1%, 100%, 94.2%, and 88.70% were achieved on dataset 1 (dataset IIIb: three subjects), dataset 2 (dataset III: one subject), dataset 3 (dataset 2b: 9 subjects) and dataset 4 (OpenBMI dataset: 12 subjects) respectively.

The WFF technique shows high faculty to make features more discriminate and could be a valuable and worthwhile approach for the MI-EEG-based BCI system. The experimental results corroborate that the suggested method outperforms the existing methods and has the benefit of enhanced classification performance.

These findings provide a new perspective on developing BCI systems with superior performance and efficiency. This study, which used the LSVM classifier, reveals the possibility to transform classification problems, with the WFF technique, into more linearly separable ones while keeping the same data dimension without using kernel functions commonly used in the SVM classifier. The WFF technique used in this work applies the 'tan' function, a nonlinear and periodical function to features polynomial transformation. This allows increasing the possibility to separate linearly different regions in the classification problem domain. In that sense, more functions can be studied to transform features to a new domain more linearly separable. It is worthful to note that using classical machine learning, compared to deep learning, when using proper features can give better results compared to the results given by the deep learning. This claim is verified by this work.

This study reveals an important result. The information about the MI tasks can be gained from small number of electrodes if we use proper features. Using small electrodes, make the user more comfortable, increase the response time leading to low power consumption.

Acknowledgment

The authors would like to acknowledge the Institute for Knowledge Discovery (Laboratory of Brain-Computer Interfaces), Graz University of Technology, for providing the dataset online. (https://www.bbci.de/competition). The acknowledge goes also to the GigaScience repository (GigaDB) that makes datasets available publicly(https://gigadb.org/dataset/100542).

References

[1] Altaheri H., Muhammad G., Alsulaiman M., Amin S., and et al., "Deep Learning Techniques for Classification of Electroencephalogram (EEG) Motor Imagery (MI) Signals: A Review," *Neural Computing and Applications*, vol. 35, pp. 14681-14722, 2023. https://doi.org/10.1007/s00521-021-06352-5

[2] Bashashati H., Ward R., Birch G., and Bashashati A., "Comparing Different Classifiers in Sensory Motor Brain Computer Interfaces," *PLoS ONE*, vol. 10, no. 6, pp. 1-17, 2015. https://doi.org/10.1371/journal.pone.0129435

[3] Bhattacharyya S., Khasnobish A., Chatterjee S., Konar A., and Tibarewala D., "Performance Analysis of LDA, QDA and KNN Algorithms in Left-Right Limb Movement Classification from EEG Data," *in Proceedings of the International Conference on Systems in Medicine and Biology*, Kharagpur, pp. 126-131, 2010. https://ieeexplore.ieee.org/document/5735358

[4] Blankertz B., Muller K., Curio G., Vaughan T., and et al., "The BCI Competition 2003: Progress and Perspectives in Detection and Discrimination of EEG Single Trials," *IEEE Transactions on Biomedical Engineering*, vol. 51, no. 6, pp. 1044-1051, 2004. https://pubmed.ncbi.nlm.nih.gov/15188876/

[5] Blankertz B., Muller K., Krusienski D., Schalk G., and et al., "The BCI Competition III: Validating Alternative Approaches to Actual BCI Problems," *IEEE Transactions on Neural Systems and Rehabilitation Engineering*, vol. 14, no. 2, pp. 153-159, 2006. https://doi.org/10.1109/TNSRE.2006.875642

[6] Brodu N., Lotte F., and Lecuyer A., "Comparative Study of Band-Power Extraction Techniques for Motor Imagery Classification," *in Proceedings of the IEEE Symposium on Computational Intelligence, Cognitive Algorithms, Mind, and Brain*, Paris, pp. 1-6, 2011. https://ieeexplore.ieee.org/document/5952105

[7] Brodu N., Lotte F., and Lecuyer A., "Exploring Two Novel Features for EEG-based Brain-Computer Interfaces: Multifractal Cumulants and Predictive Complexity," *Neurocomputing*, vol. 79, pp. 87-94, 2012. https://doi.org/10.1016/j.neucom.2011.10.010

[8] Buskila Y., Bellot-Saez A., and Morley J.,

"Generating Brain Waves, the Power of Astrocytes," *Frontiers in Neuroscience*, vol. 13, pp. 1-10, 2019. DOI: 10.3389/fnins.2019.01125

[9] Chen C., Yu X., Belkacem A., Lu L., and et al., "EEG-based Anxious States Classification Using Affective BCI-based Closed Neurofeedback System," *Journal of Medical and Biological Engineering*, vol. 41, pp. 155-164, 2021. https://doi.org/10.1007/s40846-020-00596-7

[10] Chen W., Wang X., and Zhang T., "Research of Discrimination between Left and Right Hand Motor Imagery EEG Patterns Based on Tunable Q-Factor Wavelet Transform," *Journal of Electronics and Information Technology*, vol. 41, no. 3, pp. 530-536, 2019. https://www.jeit.ac.cn/en/article/doi/10.11999/JEIT171191

[11] Chowdary M., Anitha J., and Hemanth D., "Emotion Recognition from EEG Signals Using Recurrent Neural Networks," *Electronics*, vol. 11, no. 15, pp. 1-20, 2022. https://doi.org/10.3390/electronics11152387

[12] Coyle D., Prasad G., and McGinnity T., "A Time-Frequency Approach to Feature Extraction for a Brain-Computer Interface with a Comparative Analysis of Performance Measures," *EURASIP Journal on Advances in Signal Processing*, vol. 19, pp. 3141-3151, 2005. https://doi.org/10.1155/ASP.2005.3141

[13] Dagdevir E. and Tokmakci M., "Optimization of Preprocessing Stage in EEG Based BCI Systems in Terms of Accuracy and Timing Cost," *Biomedical Signal Processing and Control*, vol. 67, pp. 102548, 2021. https://doi.org/10.1016/j.bspc.2021.102548

[14] Han Y., Wang B., Luo J., Li L., and Li X., "A Classification Method for EEG Motor Imagery Signals Based on Parallel Convolutional Neural Network," *Biomedical Signal Processing and Control*, vol. 71, pp. 103190, 2021. https://doi.org/10.1016/j.bspc.2021.103190

[15] Jang T., Kim B., Yang Y., Lim W., and Oh D., "Motor-Imagery EEG Signal Classification Using Position Matching and Vector Quantisation," *International Journal of Telemedicine and Clinical Practices*, vol. 1, no. 4, pp. 306-313, 2016. https://doi.org/10.1504/IJTMCP.2016.078426

[16] Kant P., Laskar S., Hazarika J., and Mahamune R., "CWT Based Transfer Learning for Motor Imagery Classification for Brain Computer Interfaces," *Journal of Neuroscience Methods*, vol. 345, pp. 108886, 2020. https://doi.org/10.1016/j.jneumeth.2020.108886

[17] Khasnobish A., Bhattacharyya S., Konar A., and Tibarewala D., "K-Nearest Neighbor Classification of Left-Right Limb Movement Using EEG Data," *in Proceedings of the 2nd International Conference on Biomedical Engineering and Assistive Technologies*, Punjab, pp. 1-6, 2010. https://www.academia.edu/20886132/K_Nearest_neighbor_classification_of_left_right_limb_movement_using_EEG_data

[18] Lee D., Park S., and Lee S., "Improving the Accuracy and Training Speed of Motor Imagery Brain-Computer Interfaces Using Wavelet-based Combined Feature Vectors and Gaussian Mixture Model-Supervectors," *Sensors*, vol. 17, no. 10, pp. 1-18, 2017. https://doi.org/10.3390/s17102282

[19] Lee M., Kwon O., Kim Y., Kim H., and et al., "Supporting Data for EEG Dataset and OpenBMI Toolbox for three BCI Paradigms: An Investigation into BCI Illiteracy," *GigaScience*, vol. 8, no. 5, pp. 1-16, 2019. https://doi.org/10.1093/gigascience/giz002

[20] Leeb R., Brunner C., Muller-Putz G., Schlogl A., and Pfurtscheller G., "BCI Competition 2008-Graz Data Set B," *Graz University of Technology*, vol. 16, pp. 1-6, 2008. https://www.bbci.de/competition/iv/desc_2b.pdf

[21] Liu A., Chen K., Liu Q., Ai Q., and et al., "Feature Selection for Motor Imagery EEG Classification Based on Firefly Algorithm and Learning Automata," *Sensors*, vol. 17, no. 11, pp. 1-15, 2017. https://doi.org/10.3390/s17112576

[22] Liu C., Zhao H., Li C., and Wang H., "CSP/SVM-based EEG Classification of Imagined Hand Movements," *Journal of Northeast University*, vol. 31, no. 8, pp. 1098-1101, 2010. https://xuebao.neu.edu.cn/natural/EN/Y2010/V31/I8/1098

[23] Liu X., Xiong S., Wang X., Liang T., and et al., "A Compact Multi-Branch 1D Convolutional Neural Network for EEG-based Motor Imagery Classification," *Biomedical Signal Processing and Control*, vol. 81, pp. 104456, 2023. https://doi.org/10.1016/j.bspc.2022.104456

[24] Lotte F., Lecuyer A., Lamarche F., and Arnaldi B., "Studying the Use of Fuzzy Inference Systems for Motor Imagery Classification," *IEEE Transactions on Neural Systems and Rehabilitation Engineering*, vol. 15, no. 2, pp. 322-324, 2007. https://doi.org/10.1109/TNSRE.2007.897032

[25] Lu N., Li T., Ren X., and Miao H., "A Deep Learning Scheme for Motor Imagery Classification Based on Restricted Boltzmann Machines," *IEEE Transactions on Neural Systems and Rehabilitation Engineering*, vol. 25, no. 6, pp. 566-576, 2017. https://ieeexplore.ieee.org/document/7546909

[26] Malan N. and Sharma S., "Motor Imagery EEG Spectral-Spatial Feature Optimization Using Dual-Tree Complex Wavelet and Neighbourhood Component Analysis," *IRBM*, vol. 43, no. 3, pp. 198-209, 2021.

https://doi.org/10.1016/j.irbm.2021.01.002

[27] Mebarkia K. and Reffad A., "Multi Optimized SVM Classifiers for Motor Imagery Left and Right Hand Movement Identification," *Australasian Physical and Engineering Sciences in Medicine*, vol. 42, pp. 949-958, 2019. https://doi.org/10.1007/s13246-019-00793-y

[28] Meng J., Zhang S., Bekyo A., Olsoe J., and et al., "Noninvasive Electroencephalogram Based Control of a Robotic Arm for Reach and Grasp Tasks," *Scientific Reports*, vol. 6, pp. 1-15, 2016. https://doi.org/10.1038/srep38565

[29] Mishuhina V. and Jiang X., "Feature Weighting and Regularization of Common Spatial Patterns in EEG-based Motor Imagery BCI," *IEEE Signal Processing Letters*, vol. 25, no. 6, pp. 783-787, 2018. https://doi.org/10.1109/LSP.2018.2823683

[30] Mohammadi E., Daneshmand P., and Khorzooghi S., "Electroencephalography-based Brain-Computer Interface Motor Imagery Classification," *Journal of Medical Signals and Sensors*, vol. 12, no. 1, pp. 40-47, 2021. https://doi.org/10.4103/jmss.JMSS_74_20

[31] Ocak H., "Optimal Classification of Epileptic Seizures in EEG Using Wavelet Analysis and Genetic Algorithm," *Signal Processing*, vol. 88, no. 7, pp. 1858-1867, 2008. https://doi.org/10.1016/j.sigpro.2008.01.026

[32] Pfurtscheller G. and Neuper C., "Motor Imagery and Direct Brain-Computer Communication," *Proceedings of the IEEE*, vol. 89, no. 7, pp. 1123-1134, 2001. https://doi.org/10.1109/5.939829

[33] Pfurtscheller G., Neuper C., Schlogl A., and Lugger K., "Separability of EEG Signals Recorded During Right and Left Motor Imagery Using Adaptive Autoregressive Parameters," *IEEE Transactions on Rehabilitation Engineering*, vol. 6, no. 3, pp. 316-325, 1998. https://doi.org/10.1109/86.712230

[34] Pinheiro O., Alves L., and Souza J., "EEG Signals Classification: Motor Imagery for Driving an Intelligent Wheelchair," *IEEE Latin America Transactions*, vol. 16, no. 1, pp. 254-259, 2018. https://doi.org/10.1109/TLA.2018.8291481

[35] Reddy V. and Ravi Kumar A., "Multi-Channel Neuro Signal Classification Using Adam-based Coyote Optimization Enabled Deep Belief Network," *Biomedical Signal Processing and Control*, vol. 77, pp. 103774, 2022. https://doi.org/10.1016/j.bspc.2022.103774

[36] Reffad A. and Mebarkia K., "Motor Imagery hand Movements Recognition Using SVM Classifier and Genetic Algorithm Optimization," *in Proceedings of the 19th International Multi-Conference on Systems, Signals and Devices*, Setif, pp. 1125-1129, 2022. https://doi.org/10.1109/SSD54932.2022.9955863

[37] Rossi E., Pereira Soares S., Prystauka Y., Nakamura M., and Rothman J., "Riding the (Brain) Waves! Using Neural Oscillations to Inform Bilingualism Research," *Bilingualism: Language and Cognition*, vol. 26, no. 1, pp. 202-215, 2023. https://doi.org/10.1017/S1366728922000451

[38] Salimpour S., Kalbkhani H., Seyyedi S., and Solouk V., "Stockwell Transform and Semi-Supervised Feature Selection from Deep Features for Classification of BCI Signals," *Scientific Reports*, vol. 12, pp. 1-19, 2022. https://doi.org/10.1038/s41598-022-15813-3

[39] Sidaoui B. and Sadouni K., "Epilepsy Seizure Prediction from EEG Signal Using Machine Learning Techniques," *Advances in Electrical and Computer Engineering*, vol. 23, no. 2, pp. 47-54, 2023. https://doi.org/10.4316/AECE.2023.02006

[40] Smrdel A., "Use of Common Spatial Patterns for Early Detection of Parkinson's Disease," *Scientific Reports*, vol. 12, pp. 1-10, 2022. https://doi.org/10.1038/s41598-022-23247-0

[41] Tabar Y. and Halici U., "A Novel Deep Learning Approach for Classification of EEG Motor Imagery Signals," *Journal of Neural Engineering*, vol. 14, no. 1, pp. 016003, 2017. https://doi.org/10.1088/1741-2560/14/1/016003

[42] Tibrewal N., Leeuwis N., and Alimardani M., "Classification of Motor Imagery EEG Using Deep Learning Increases Performance in Inefficient BCI Users," *PLoS ONE*, vol. 17, no. 7, pp. 1-18, 2022. https://doi.org/10.1371/journal.pone.0268880

[43] Too J., Abdullah A., and Saad N., "Classification of Hand Movements Based on Discrete Wavelet Transform and Enhanced Feature Extraction," *International Journal of Advanced Computer Science and Applications*, vol. 10, no. 6, pp. 83-89, 2019. https://doi.org/10.14569/IJACSA.2019.0100612

[44] Wan Ismail W., Hanif M., and Hamzah N., "Human Emotion Detection via Brain Waves Study by Using Electroencephalogram (EEG)," *International Journal of Advanced Science, Engineering and Information Technology*, vol. 6, no. 6, pp. 1005-1011, 2016. https://ijaseit.insightsociety.org/index.php/ijaseit/article/view/1072/pdf_297

[45] You Y., Chen W., and Zhang T., "Motor Imagery EEG Classification Based on Flexible Analytic Wavelet Transform," *Biomedical Signal Processing and Control*, vol. 62, pp. 102069, 2020. https://doi.org/10.1016/j.bspc.2020.102069

[46] Zhang W., Huang R., and Ye L., "Evaluation of Emission Reduction Performance of Power Enterprises Based on Least Squares Support Vector Machine," *The International Arab Journal of Information Technology*, vol. 21, no. 5, pp. 854-865, 2024. https://doi.org/10.34028/iajit/21/5/7

[47] Zhong M., Lotte F., Girolami M., and Lecuyer A.,

"Classifying EEG for Brain Computer Interfaces Using Gaussian Processes," *Pattern Recognition Letters*, vol. 29, no. 3, pp. 354-359, 2008. https://doi.org/10.1016/j.patrec.2007.10.009

Abdel Fateh Doudou is a doctoral student in Automation and Industrial Informatics at Setif 1 University-Ferhat Abbas. In 2019, he received his Master's degree in Automation and Industrial Informatics from the same university. He joined the Department of Electrotechnics in 2020 and has been a member of the Automation Laboratory at Setif 1 University-Ferhat Abbas since then. His research interests include Signal Processing, Pattern Recognition, Classification, and Feature Selection.

Aicha Reffad is a Lecturer and Researcher at the Electrotechnics Department, Setif 1 University, Algeria. Received the Ph.D. degree in collaboration with the Laboratory for Engineering of Neuromuscular System in Torino, Italy in 2009. During the year 2012, she worked in collaboration at the Department of Rehabilitation and Prevention Engineering RPE in Germany. She is interested in Signal and Image Processing for Biomedical Engineering (diagnosis and rehabilitation); Brain Computer Interface (BCI) and Control.

Kamel Mebarkia is a Lecturer and Researcher at the Electronics Department, Setif 1 University, Algeria. Received the Magister diploma from the same Department in 2005. In 2014, he received Ph.D. degree working on the EMG field in collaboration with Helmholtz institute, Aachen University. He is interested in Signal and Image Processing in Biomedical Engineering (diagnosis and rehabilitation); Signal Modeling, Analyses and Parametrization; Brain Computer Interface (BCI) and Control; Information Theory and Communications; Artificial Intelligence and Machine Learning.